

Article

Not peer-reviewed version

Near-Infrared Phosphorescence of the Raman Photogenerated Singlet Oxygen

[Aristides Marciano Olaizola](#) *

Posted Date: 6 June 2024

doi: 10.20944/preprints202406.0405.v1

Keywords: Raman spectroscopy; singlet oxygen photoexcitation; phosphorescence of singlet oxygen



Preprints.org is a free multidiscipline platform providing preprint service that is dedicated to making early versions of research outputs permanently available and citable. Preprints posted at Preprints.org appear in Web of Science, Crossref, Google Scholar, Scilit, Europe PMC.

Copyright: This is an open access article distributed under the Creative Commons Attribution License which permits unrestricted use, distribution, and reproduction in any medium, provided the original work is properly cited.

Disclaimer/Publisher's Note: The statements, opinions, and data contained in all publications are solely those of the individual author(s) and contributor(s) and not of MDPI and/or the editor(s). MDPI and/or the editor(s) disclaim responsibility for any injury to people or property resulting from any ideas, methods, instructions, or products referred to in the content.

Article

Near-Infrared Phosphorescence of the Raman Photogenerated Singlet Oxygen

Aristides Marcano Olaizola

Division of Physics, Engineering, Mathematics, and Computer Science, Delaware State University, 1200 North DuPont Highway, Dover, DE 19901, USA; amarcano@desu.edu

* Correspondence: amarcano@desu.edu; Tel.: 001 302 857 6690

Abstract: We report on the phosphorescence of singlet oxygen photogenerated through a stimulated Raman process. Nanosecond radiation in the green spectral region focused on hexane induces a Raman transition of the dissolved in the solvent oxygen molecules toward the singlet oxygen state producing a Stokes signal in the near infrared. The excited oxygen relaxes to ground emitting an infrared photon at 1269 nm. While the Stokes signal's wavelength changes with the pumping light's wavelength, the wavelength of the phosphorescent photon remains unaltered. The result confirms previously reports on stimulated Raman excitation of singlet oxygen.

Keywords: Raman spectroscopy; singlet oxygen photoexcitation; phosphorescence of singlet oxygen

1. Introduction

Singlet oxygen ($^1\text{O}_2$) is a reactive oxygen species (ROS) corresponding to the molecular oxygen first excited electronic state. $^1\text{O}_2$ is highly electrophilic. This property is the base for its broad use in bacteria [1], viruses [2], and fungi [3] inactivation, photodynamic treatment of cancer [4], protein studies [5], environment conservation [6], among other remarkable applications in photochemistry, photobiology, and photomedicine [7]. Quantum mechanics selection rules prohibit a direct one-photon $^1\text{O}_2$ photoexcitation. Photosensitizing is the standard procedure for its production. A photosensitizer absorbs energy from visible photons and retransmits it toward surrounding oxygen molecules through a radiation-less relaxation process, exciting the $^1\text{O}_2$ state. The procedure adds complexity and undesirable secondary effects, such as excessive long-lasting photosensitivity.

We have recently described a new approach that does not require photosensitizers based on the stimulated Raman effects [8,9]. Nanosecond laser radiation in the blue spectral region induces $^1\text{O}_2$ Raman excitation, emitting a Stokes component in the red spectral region. In this work, we validate the finding demonstrating $^1\text{O}_2$ Raman photogeneration by directly detecting its phosphorescence. $^1\text{O}_2$ exhibits a weak phosphorescence in the near-infrared (NIR) at 1269 nm, corresponding to its relaxation toward the ground state. Krasnovsky reported the 1269 nm $^1\text{O}_2$ phosphorescence as a direct method of its detection in 1976 [10]. Since then, the near-infrared luminescence has been widely used as the standard procedure for $^1\text{O}_2$ detection [11–14]. NIR high-sensitivity detection methods are required to register the weak $^1\text{O}_2$ phosphorescence.

In this work, we report on NIR phosphorescence detection of Raman photogenerated $^1\text{O}_2$. As samples, we use hexane and methanol, which contain relatively large dissolved oxygen concentrations. We irradiate the sample using nanosecond radiation in the green region of the spectra (500 – 540 nm). We use long-pass glass filters and a double-grating monochromator to remove the contribution from the solvent vibrational modes. A germanium detector detects the NIR signal. The $^1\text{O}_2$ Stokes component is expected in the 830 – 880 nm spectral region. A second overtone from the solvent stretching mode is expected in the 882–1015 nm region. The position of these peaks depends on the value of the pumping wavelength, which corresponds to Raman Stokes signals. We report on detecting weak peaks at 1269 nm, which we associate with $^1\text{O}_2$ phosphorescence. When changing the

pump wavelength, the peak wavelength remains the same, corresponding to a luminescence signal. We use this fact as a criterion for identification and separation from the Stokes components. We report that the phosphorescence peak amplitude changes significantly when scanning the pump wavelength. The signal reaches its maximal value for the pumping wavelength at 520 nm, which should correspond to conditions for a more efficient Raman $^1\text{O}_2$ photogeneration.

2. Materials and Methods

Figure 1 shows a simplified schematic of the experiment. An optical parametric oscillator (OPO, OPOTEK, Carlsbad, CA, US) provides 5-nanosecond excitation in the blue-green region (500-540 nm) with an average energy per pulse of 20 mJ. A beam-splitter B deviates part of the light toward a reference detector. The bandpass filter BPF (375-700 nm) transmits the green radiation and depletes any residual NIR light from the OPO. A 20-cm focal length lens L_1 focuses the pump light onto a 10-cm path-length glass cuvette containing the sample. A long-pass filter LPF1 with a cut-off wavelength of 610 nm depletes the pumping light and most of the visible components of the solvent. Due to Raman nonlinear refraction, the beam transmitted through the sample exhibits a central spot and a colored ring structure. The central spot contains remnants of the pumping light and solvent Stokes contributions, including the weak NIR components. The ring structure also has contributions from the pumping beam and Stokes peaks but in less proportions than the NIR signals. We use the light blocker D to remove the central spot without affecting the ring structure's light.

The lens L_2 focuses the transmitted ring light into a double grating spectrometer (Cornerstone 260 $\frac{1}{4}$ m extended range, Newport, Irvine, CA, US). At the spectrometer's entrance, we place a long-pass filter with a cut-on wavelength of 850 nm, which depletes any visible light contribution. We scan the spectrometer in the region 800 nm- 1400 nm. At the output of the spectrometer, we use a Germanium-biased photodiode (Thorlabs DET50B2, Newton, NJ, US) with a responsivity around 0.6 A/W in the 1200-1300 region. The detector signal is amplified by a current amplifier (SR570, Stanford Research Systems, Stanford, CA, US) and sent toward a digital oscilloscope (TDS 3052, Tektronix, Beaverton, OR, US) for averaging and display. We use aerated pure hexane and methanol in 10-cm glass cuvettes as samples. The sample exhibits dissolved oxygen concentration about one order of magnitude larger than the water's.

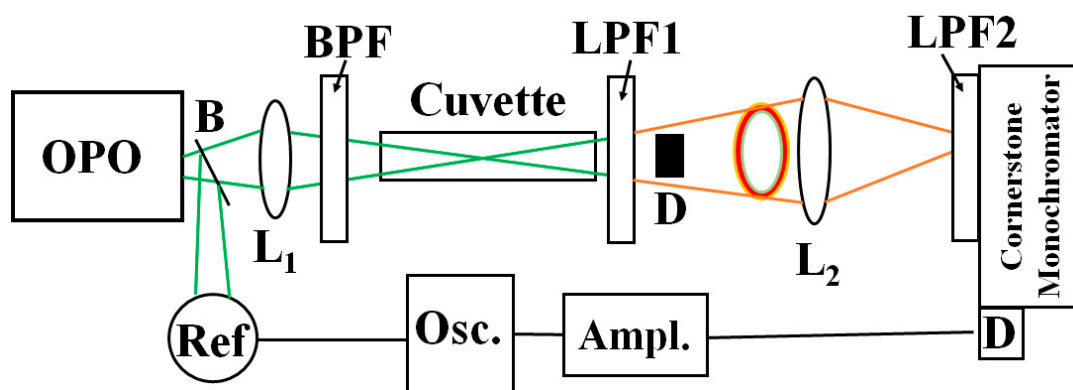


Figure 1. Schematic of the experimental set-up showing the optical parametric oscillator (OPO), a beam-splitter B, a reference detector Ref, lenses L_1 and L_2 , a band pass filter BPF, the sample cuvette, long-pass filters LPF1 and LPF2, beam blocker D, a double grating spectrometer, a germanium detector D, a current amplifier, and an oscilloscope.

3. Results and Discussion

Figure 2 shows the spectra detected in the IR region 1200-1400 nm for the hexane sample when pumping at 520 nm (red crossed circles). The peak corresponds to the $^1\text{O}_2$ phosphorescence peak at 1269 nm. The red solid line interprets the data as a Gaussian peak centered at 1269 nm with a Gaussian

width of 30 nm. We compare this peak with the Stokes signals generated by the solvent molecules' stretching modes and the Stokes signals corresponding to the $^1\text{O}_2$ photoexcitation. One fundamental difference between these signals is that all Stokes components should shift when shifting the pump wavelength. Meanwhile, the $^1\text{O}_2$ phosphorescence signal must remain at 1269 nm for all pumping wavelengths.

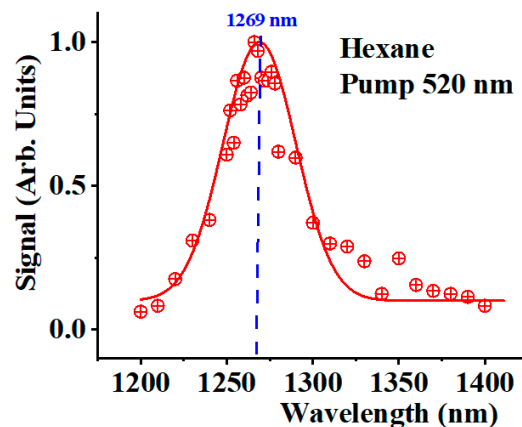


Figure 2. $^1\text{O}_2$ Phosphorescence spectrum obtained for hexane when pumping at 520 nm. The solid line is an interpretation of the data as a Gaussian peak centered at 1269 nm.

The Raman stretching mode of hexane is around 2940 cm^{-1} . A second overtone of the vibration occurs in the NIR. Table 1 provides the values of the second overtone of this fundamental solvent vibrational mode when pumping at 500, 520, and 540 nm (see column 2 in Table 1). The third column of the same table shows the expected values of the NIR Stokes components corresponding to $^1\text{O}_2$ Raman photoexcitation. Due to their proximity and the limited spectrometer's spectral resolution, both signals combine into a single Stokes peak that shifts when the pumping wavelength changes. Meanwhile, the $^1\text{O}_2$ phosphorescence peak should remain unaltered (fourth column in Table 1). The experiments confirm this fact.

Table 1. Wavelengths of the 2nd overtone of the hexane stretching mode, $^1\text{O}_2$ Stokes, and $^1\text{O}_2$ phosphorescence for different pump wavelengths.

Pump wavelength (nm)	2nd Overtone (nm)	$^1\text{O}_2$ Stokes (nm)	$^1\text{O}_2$ Phosphorescence (nm)
500	894	825	1269
520	960	881	1269
540	1031	940	1269

Figure 3a shows the spectra detected in the NIR region 800-1400 nm for the hexane sample when pumping at 500 nm (blue crossed circles), 520 nm (red crossed squares), and 540 nm (green open stars). We observe a peak that shifts when changing the pumping wavelength corresponding to a Stokes signal. This peak includes the two components. Part of the signal corresponds to the second overtone of the stretching vibration of the solvent molecule. The observed peaks also include contributions from the Stokes signals generated during the Raman excitation of $^1\text{O}_2$.

Figure 3b shows details of the spectra in the region 1200 nm-1400 nm. The plot shows the $^1\text{O}_2$ phosphorescence peak at 1269 nm. When changing the pumping wavelength, the amplitude of this peak changes, but its position does not change, confirming its interpretation as a signal of phosphorescence origin, which must be the same for any pumping wavelength. The signals in Figure 3b are measured in the same arbitrary units of Figure 3a. Thus, the phosphorescence signal is between three orders to two orders of magnitude smaller than the Stokes ones. The phosphorescence signal amplitude strongly depends on the pump wavelength value, making its detection challenging.

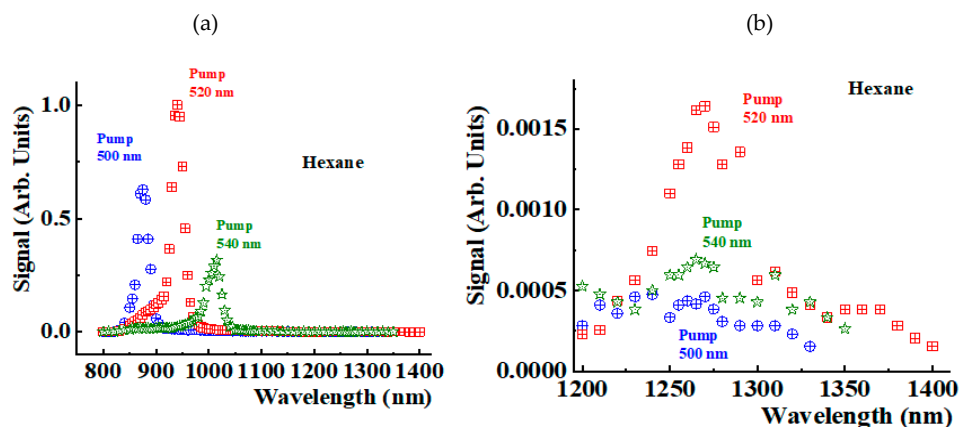


Figure 3. (a) NIR Raman spectra obtained for hexane when pumping at 500 nm (blue crossed circles), 520 nm (red crossed squares), and 540 nm (green stars); (b) Details of the spectra in the region 1200-1400 nm.

We have conducted similar experiments in methanol. Figure 4a shows the NIR spectra of methanol in the spectral region 1200-1350 nm when pumping at 520 nm. We detected a peak around 1270 nm with a significant background contribution from the solvent. The signal was about one order of magnitude smaller than the hexane phosphorescence. Figure 4b shows a similar experiment conducted in methanol when pumping at 410 nm. Despite the noisy level, we could still detect a $^1\text{O}_2$ phosphorescence signal around 1270 nm, about 15% larger than the solvent background contribution.

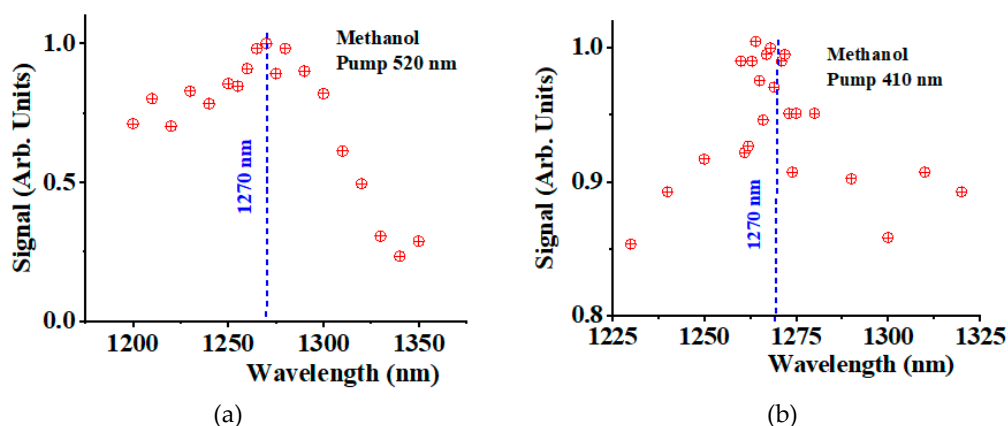


Figure 4. (a) NIR phosphorescence spectra obtained for methanol when pumping at 520 nm in the region 1200-1350 nm; (b) NIR phosphorescence spectra obtained for methanol when pumping at 410 nm in the region 1225-1325 nm.

5. Conclusions

We demonstrate the phosphorescence at 1269 nm of Raman photogenerated of $^1\text{O}_2$ without using photosensitizers in hexane and methanol. We show that the signal remains at 1269 nm even when changing the pumping wavelength, as expected for a luminescent signal. The behavior is remarkably different for any Stokes components generated in the process, for which wavelength shifts when changing the pumping wavelength.

Funding: The research was sponsored by the Air Force Office of Scientific Research and was accomplished under Grant Number W911NF-23-1-0245. The views and conclusions are those of the authors and should not be interpreted as representing the official policies, either expressed or implied, of the Air Force Office of Scientific Research or the US Government. The US Government is authorized to reproduce and distribute reprints for

Government purposes, notwithstanding any copyright notation herein. The authors also acknowledge the support of the US National Science Foundation (NSF PREM Award 2122158). Mention of trade names or commercial products in this publication is solely for the purpose of providing specific information and does not imply recommendation or endorsement by the U.S. Department of Agriculture (USDA). The USDA is an equal opportunity provider and employer.

Conflicts of Interest: "The author declares no conflicts of interest."

References

1. Dahl, T.A.; Midden, W.R.; Hartman, P.E. Comparison of killing of gram-negative and gram-positive bacteria by pure singlet oxygen. *J. Bacteriol* **1989**, *171*, 2188-2194. <https://doi.org/10.1128/jb.171.4.2188-2194.1989>.
2. Sobotta, L.; Skupin-Mrugalska, P.; Miellecarek, J.; Goslinski, T.; Balzarini, J. Photosensitizers Mediated Photodynamic Inactivation against Virus Particles. *Mini Rev. Med. Chem.* **2015**, *15*(6), 503-521.
3. Preuß, A.; Saltsman, I.; Mahammed, A.; Pfitzner, M.; Goldberg, I.; Gross, Z.; Röder, B. Photodynamic inactivation of mold fungi spores by newly developed charged corroles. *J. Photochem. Photobiol. B: Bio.* **2014**, *113*(5), 39-46. <https://doi.org/10.1016/j.jphotobiol.2014.02.013>.
4. Dougherty, T.J.; Gomer, C.J.; Henderson, B.W.; Jori, G.; Kessel, D.; Korbek, M.; Moan, J.; Peng, Q. "Photodynamic Therapy". *JNCI: J. Nat. Cancer Inst.* **1998**, *90* (12), 889-905. <http://dx.doi.org/10.1093/jnci/90.12.889>.
5. Beerermann, A.E.; Jay, D.G. "Chromophore-Assisted Laser Inactivation of Cellular Proteins". *Methods Cell Bio.* **1994**, *44*, 715-732. [http://dx.doi.org/10.1016/s0091-679x\(08\)60940-1](http://dx.doi.org/10.1016/s0091-679x(08)60940-1).
6. Wang, Y.; Lin, Y.; He, S.; Wu, S.; Yang, C. Singlet Oxygen: Properties, generation, detection, and environmental applications. *J. Hazardous Mat.* **2024**, *461*, 132538. <https://doi.org/10.1016/j.jhazmat.2023.132538>.
7. *Singlet Oxygen: Applications in Biosciences and Nanosciences - Comprehensive Series in Photochemical & Photobiological Sciences*, Volume 14, 1st ed.; S. Nonell, C. Flors, editors. Cambridge, UK: Royal Society of Chemistry, Thomas Graham House, 2016.
8. Marcano Olaizola, A.; Kingsley, D.; Kuis, R.; A. Johnson, A. Stimulated Raman Generation of Aqueous Singlet Oxygen without Photosensitizers. *J. Photochem. Photobiol. B: Bio* **2022**, *235*, 112562. <https://doi.org/10.1016/j.jphotobiol.2022.112562>.
9. Marcano Olaizola, A.; Zerrad, A.; Jenneto, F.; Kingsley, D. "Confirming the Stimulated Raman Origin of Singlet-Oxygen Photogeneration". *J. Raman Spectros.* **2024**, *55*, 58-64. <https://doi.org/10.1002/jrs.6615>.
10. Krasnovskii, A.A. Fotosensibilizirovannaia liuminestsentsiia singletnogo kisloroda v rastvore [Photosensitized luminescence of singlet oxygen in solution]. *Biofizika.* **1976**, *21*(4), 748-749. Russian. PMID: 1009166.
11. Khan, A.U. Direct spectroscopic observation of 1.27 μm and 1.58 μm emission of singlet ($^1\Delta_g$) molecular oxygen in chemically generated and dye-photosensitized liquid solutions at room temperature. *Chem. Phys. Lett.* **1980**, *72*, 112-114. [https://doi.org/10.1016/0009-2614\(80\)80252-1](https://doi.org/10.1016/0009-2614(80)80252-1).
12. Adam, W.; Kazakov, D.V.; Kazakov, V.P. Singlet oxygen chemiluminescence in peroxide reactions. *Chem. Rev.* **2005**, *105*, 3371-3387. <https://doi.org/10.1021/cr0300035>
13. Ossola, R.; Jönsson, O.M.; Moor, K.; McNeill, K. Singlet Oxygen quantum yields in environmental waters. *Chem. Rev.* **2021**, *121*, 4100-4146. <https://doi.org/10.1021/acs.chemrev.0c00781>.
14. Davis, C.A.; McNeill, K.; Janssen E.M.I. Non-singlet oxygen kinetic solvent isotope effects in aquatic photochemistry. *Environ. Sci. Technol.* **2018**, *52*, 9908-9916. <https://doi.org/10.1021/acs.est.8b01512>.

Disclaimer/Publisher's Note: The statements, opinions and data contained in all publications are solely those of the individual author(s) and contributor(s) and not of MDPI and/or the editor(s). MDPI and/or the editor(s) disclaim responsibility for any injury to people or property resulting from any ideas, methods, instructions or products referred to in the content.